Representation of Summertime Low-Level Jets in the Central United States by the NCEP–NCAR Reanalysis

CHRISTOPHER J. ANDERSON AND RAYMOND W. ARRITT

Department of Agronomy, Iowa State University, Ames, Iowa

(Manuscript received 7 June 1999, in final form 13 March 2000)

ABSTRACT

Reanalysis datasets that are produced by assimilating observations into numerical forecast models may contain unrealistic features owing to the influence of the underlying model. The authors have evaluated the potential for such errors to affect the depiction of summertime low-level jets (LLJs) in the NCEP–NCAR reanalysis by comparing the incidence of LLJs over 7 yr (1992–98) in the reanalysis to hourly observations obtained from the NOAA Wind Profiler Network. The profiler observations are not included in the reanalysis, thereby providing an independent evaluation of the ability of the reanalysis to represent LLJs.

LLJs in the NCEP–NCAR reanalysis exhibit realistic spatial structure, but strong LLJs are infrequent in the lee of the Rocky Mountains, causing substantial bias in LLJ frequency. In this region the forecast by the reanalysis model diminishes the ageostrophic wind, forcing the analysis scheme to restore the ageostrophic wind. The authors recommend sensitivity tests of LLJ simulations by GCMs in which terrain resolution and horizontal grid spacing are varied independently.

1. Introduction

Many climate and weather questions remain elusive because we lack data of sufficient spatial and temporal coverage. The recent development of global reanalyses that combine general circulation model (GCM) predictions with observations presents an opportunity to address some of these questions (e.g., see Higgins et al. 1996; Mo et al. 1997). Advantages of using reanalysis output are that the data record is continuous and provides upper-air data at nonsynoptic reporting times, and that studies using the same reanalysis output have in common a quality control procedure. The availability of data at nonsynoptic times is advantageous for climate studies in the central United States, where low-level jets (LLJs) strongly influence the climate [see Stensrud (1996) and Schubert et al. (1998) for overviews and discussion]. Maximum LLJ activity occurs around 0600 UTC (Mitchell et al. 1995; Whiteman et al. 1997), implying that datasets generated from the standard radiosonde network with launches at nominal times of 0000 and 1200 UTC often fail to detect LLJs.

With the advantages of reanalysis datasets comes the risk that realism of important atmospheric phenomena might be degraded in the GCM prediction. This is especially relevant to LLJs, because the dynamics of LLJ formation may not be well represented by the GCM. This may explain, in part, the variations in GCM predictions of the spatial distribution of seasonal LLJ frequency (Helfand and Schubert 1995; Ghan et al. 1996). It is useful, therefore, to examine how closely LLJs in the reanalysis resemble observed LLJs and to document the biases in the reanalysis.

Here we evaluate LLJs in the reanalysis generated by the National Center for Environmental Prediction and the National Center for Atmospheric Research (from this point referred to simply as ''reanalysis''; Kalnay et al. 1996). Previous studies have shown that springtime LLJs in the reanalysis during 1985–89 were most frequent at night (Higgins et al. 1996), consistent with the observed nocturnal preference for LLJ formation (Blackadar 1957; Bonner 1968; Mitchell et al. 1995). The geographical pattern of springtime LLJ frequency was broadly similar to observed patterns of annual and warm season LLJ frequency found by Bonner (1968). Statistics for summertime LLJs in the reanalysis during 1985–89 also were found to be in general agreement with observational climatologies (Higgins et al. 1997). We note that in the aforementioned comparisons the reanalysis and observed data were separated by as much as two decades and were collected over different periods within the year (except for a 2-week comparison at one point in the southern Great Plains).

In the present study we evaluate the one-to-one correspondence between the reanalysis and observations

Corresponding author address: Christopher J. Anderson, Dept. of Agronomy, Iowa State University, 3010 Agronomy Hall, Ames, IA 50011-1010.
E-mail: candersn@iastate.edu

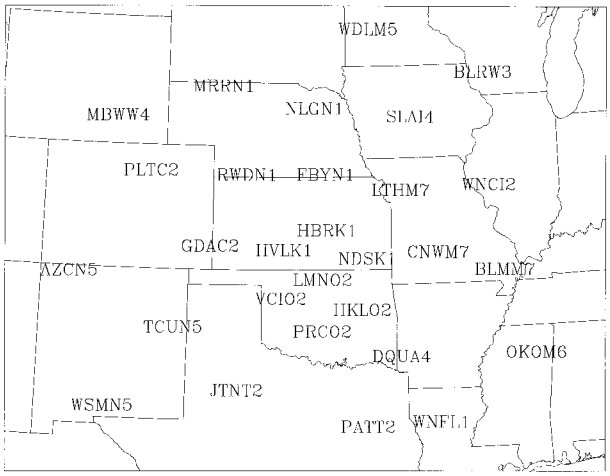

FIG. 1. Location of the 404-MHz wind profilers in the NOAA Wind Profiler Network.

from the NOAA Wind Profiler Network (NPN). Since NPN observations are not assimilated into the reanalysis, this comparison tests the reanalysis against independent data. In addition, we perform our evaluation over an entire season (JJA) for 7 yr (1992–98) so that we examine realism of LLJs in the reanalysis under a wide variety of meteorological conditions. One motivation for our study is the possibility that LLJs may be unrealistic at data-sparse times when the influence of the forecast by the reanalysis GCM is likely to be greater. Therefore we compare the performance of the reanalysis at 1200 UTC, which is one of the nominal launch times for rawinsondes over the United States, with its performance at 0600 UTC when observations included in the reanalysis are relatively sparse.

2. Data sources

a. Reanalysis

The reanalysis uses a state of the art GCM and assimilation system to produce three-dimensional atmospheric fields every 6 h (Kalnay et al. 1996). In order to generate LLJ statistics from the highest resolution reanalysis dataset available we analyze u and v wind components from the dataset having a T62 Gaussian grid (approximately 210-km grid spacing in physical space) on 28 sigma levels. Ten of the sigma levels are near or below 3000 m, assuming a standard atmospheric lapse rate (Kalnay et al. 1996). The spatial resolution is comparable to that of the NPN from which we construct our observational dataset.

b. NOAA 404-MHz wind profilers

The NPN is a network of 404-MHz Doppler radars, which are mostly located in the central United States. Typical horizontal spacing between NPN sites is approximately 200 km (Fig. 1). The hourly NPN wind measurements are consensus averages that are produced from 6-min samples made over the hour for which the observation is valid. The hourly time resolution of the NPN observations is well suited to the study of LLJs, which have a pronounced diurnal life cycle. The vertical range gates are weighted layer averages (320-m layer) that are spaced 250 m apart beginning at 500 m above ground level (Barth et al. 1994). Our NPN dataset includes observations for the years 1992–98.

The most critical limitation of our NPN dataset is that LLJs often occur below the lowest range gate (Stensrud 1996; Whiteman et al. 1997). In a recent comparison of observations from a NPN site in the southern Great Plains to high-resolution rawinsonde data (Daniel et al. 1999) the NPN detected most LLJs (the probability of detection exceeds 70%). Daniel et al. (1999) also found a tendency for LLJs in the NPN dataset to have peak wind speed less than in datasets derived from rawinsonde observations, especially LLJs that occurred below 500 m.

Another possible source of error in NPN observations is contamination of the wind measurement by migrating birds (Wilczak et al. 1995; Arritt et al. 1997). Because bird migration is seasonal, maximum error occurs during spring and fall; during summer (JJA) contamination is essentially absent (Arritt et al. 1997). Therefore, we limit our study to the summer months so that any potential bias due to bird migration is negligible.

TABLE 1. Categorical LLJ criteria from Bonner (1968).

LLJ category	Max wind speed below 1500 m	Largest decrease from the max wind speed in the layer from the height of the max to 3000 m
1	$\geq$12 m s^{-1}	$\geq$6 m s^{-1}
2	$\geq$16 m s^{-1}	$\geq$8 m s^{-1}
3	$\geq$20 m s^{-1}	$\geq$10 m s^{-1}

3. Evaluation of NCEP–NCAR reanalysis summertime LLJ frequency

a. Method

We first interpolated the reanalysis u and v wind components to the NPN sites, performing the interpolation on the reanalysis sigma levels to preserve the vertical resolution of the data. We then applied the categorical LLJ definition from Bonner (1968) to both the NPN and interpolated reanalysis wind profiles (Table 1). Notice that the categories are inclusive so that a category 3 LLJ also satisfies the criteria for a category 1 LLJ and thus is tabulated in both categories. In order to compare the depiction of weak and strong LLJs we defined exclusive LLJ categories in which the lower categories do not include events from higher categories.

Missing data in the lowest levels of the NPN observations could bias our statistics. To diminish this possibility, we adopted the approach of Mitchell et al. (1995) and computed statistics for a subset of usable profiles. We defined a usable NPN profile as one that contains at least three valid data points below 1500 m and at least four between 1500 and 3000 m, and considered only those interpolated reanalysis profiles that were simultaneous with NPN usable profiles. We computed seasonal frequency for each LLJ category (both exclusive and inclusive) at each NPN site as the ratio of the number of LLJs in that category to the number of usable profiles. Our analysis is limited to category 1 (LLJ1) and category 3 (LLJ3) LLJs. LLJ1 frequency serves as a gross measure of LLJ activity, while LLJ3 frequency relates to heavy precipitation episodes and occurrence of mesoscale convective systems (MCS; Maddox 1983; Higgins et al. 1997; Arritt et al. 1997; Anderson and Arritt 1998; Schubert et al. 1998).

b. Seasonal LLJ frequency

The NPN LLJ1 frequency at 0600 and 1200 UTC (Fig. 2) is largest in the southwestern Great Plains, decreasing from west to east and (not as abruptly) south to north. Aside from the magnitude of the maximum frequency (which is exaggerated by including only these two reporting times), the spatial characteristics are consistent with previous LLJ climatologies (Bonner 1968; Mitchell et al. 1995; Arritt et al. 1997).

We define the station bias as the difference of the 7-yr (1992–98) LLJ1 frequency at a particular NPN site from that of the reanalysis (Fig. 3). Note that the units of this measure are percent, representing a difference of percentages and not a ratio. The average bias is the sum of the station biases divided by the number of stations. In a similar manner, we compute the average NPN LLJ frequency from the station LLJ frequencies. At 0600 UTC the average bias is 0.06% (from an average NPN LLJ frequency of 15.20%), while at 1200 UTC it is −2.34% (from an average NPN LLJ frequency of 12.88%). Thus, the general tendency (average over both 0600 and 1200 UTC) is for the reanalysis to underrepresent slightly the LLJ1 frequency compared to the profilers, which themselves understate the frequency of LLJs compared to rawinsondes (Daniel et al. 1999).

The spatial pattern of LLJ1 station bias at 0600 UTC is very different from that at 1200 UTC when all but three NPN sites have negative bias. In the southern Great Plains, the station bias changes from about +5% at 0600 UTC to about −5% at 1200 UTC, whereas the station bias in the northern Great Plains is nearly constant at approximately −2%. Including observations prevents the reanalysis from assuming the model climatology; nevertheless, substantial regional bias remains.

The spatial patterns of NPN LLJ3 frequency (Fig. 4) also have features in common with previous LLJ cli-

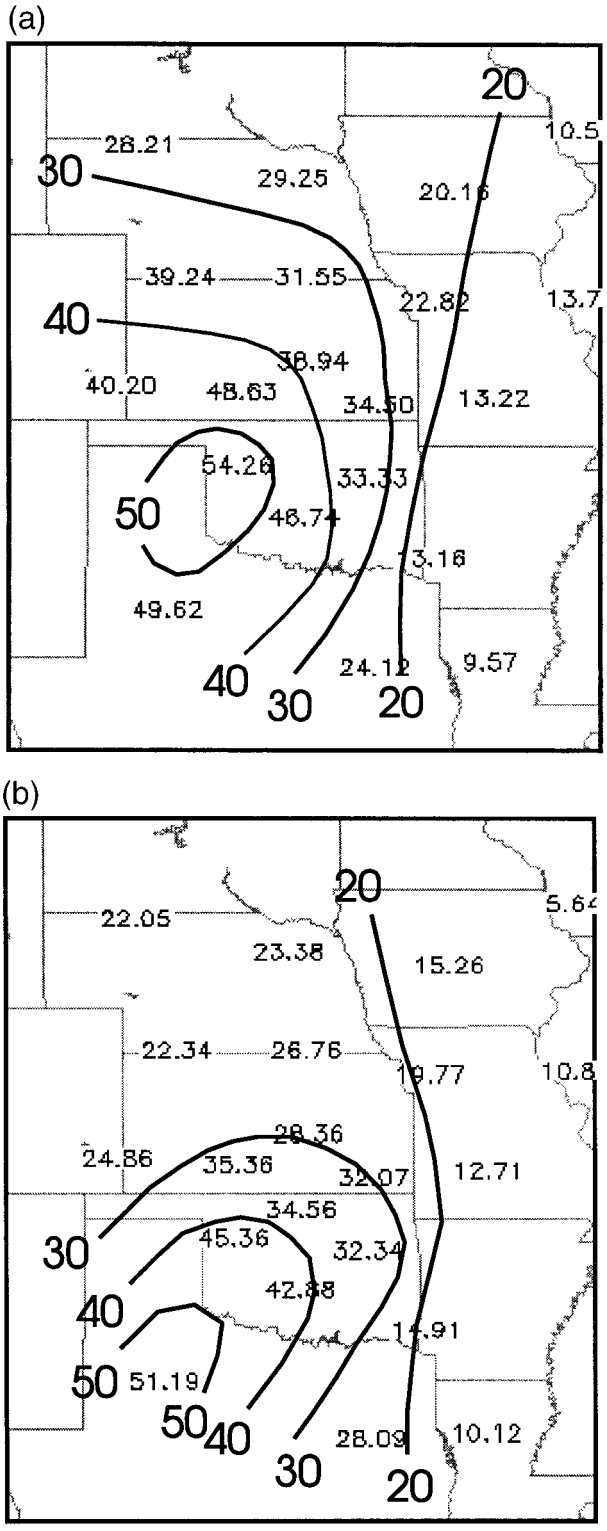

FIG. 2. NPN summertime LLJ1 frequency (1992–98) at (a) 0600 UTC and (b) 1200 UTC (contour interval is 10%).

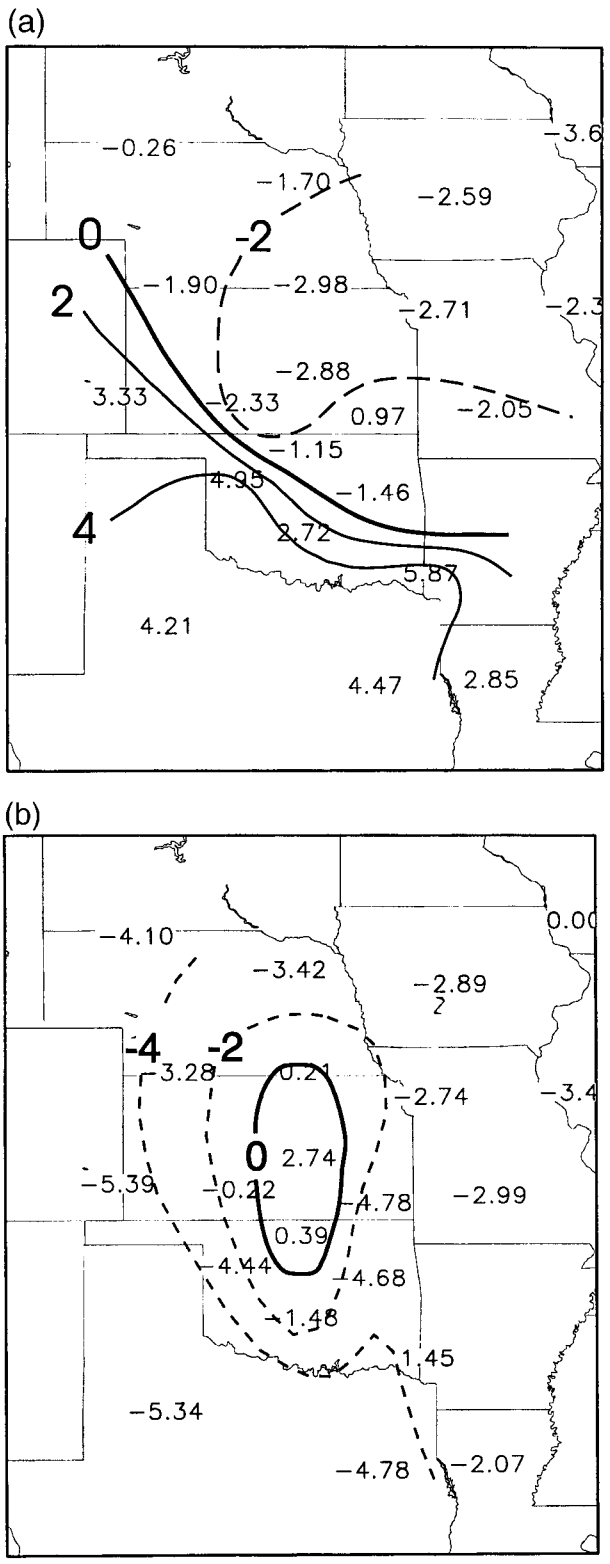

FIG. 3. Summertime LLJ1 station bias (reanalysis minus NPN) at (a) 0600 UTC and (b) 1200 UTC (contour interval is 2%; dashed lines denote negative bias).

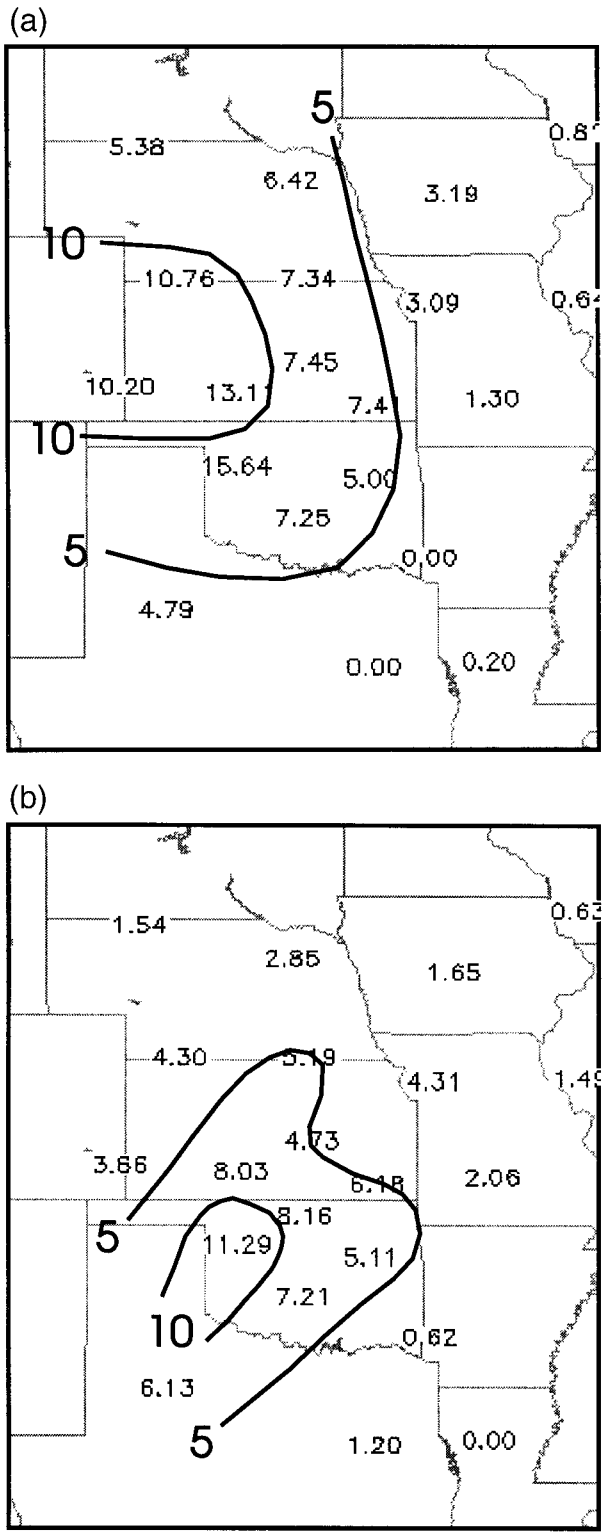

FIG. 4. NPN summertime LLJ3 frequency (1992–98) at (a) 0600 UTC and (b) 1200 UTC (contour interval is 5%).

matologies. For example, the maximum LLJ3 frequency is located in western Kansas and western Oklahoma at 0600 UTC (Bonner 1968; Mitchell et al. 1995; Arritt et al. 1997). The reanalysis, however, underrepresents LLJ3 frequency (Fig. 5). Though the negative LLJ3 station bias at 0600 UTC is somewhat larger in magnitude than at 1200 UTC, the fractional decrease relative to the NPN climatology is similar at both times. This means that the more negative bias at 0600 UTC does not necessarily imply poorer model performance. The bias may be most significant in the northern Great Plains where the bias is of opposite sign and nearly equal magnitude to the NPN station frequency, implying that the reanalysis fails to include almost all LLJ3 episodes in this region.

c. Spatial structure

Here we examine the ability of the reanalysis to represent the spatial extent of LLJs using pseudocorrelation maps for two of the NPN sites. (We use the LLJ categories in the overlapping sense.) We present maps for 0600 UTC only, since 1200 UTC maps are very similar. We constructed the maps by first selecting a reference site. We then tallied at each of the other sites the number of LLJ occurrences simultaneous with those at the reference site. The pseudocorrelation is the ratio of the simultaneous occurrences between the two sites to the total number of occurrences at the reference site.

Pseudocorrelation maps for Granada, Colorado, (GDAC2 in Fig. 1) and Slater, Iowa, (SLAI4 in Fig. 1), derived from the NPN data demonstrate the dependence of the horizontal scale of LLJs on geographical location (Figs. 6a and 7a). Spatial structure in the pseudocorrelation map for SLAI4 is consistent with the classic conception of LLJs as a relatively narrow stream (streamwise extent much larger than the transverse extent) of low-level southerly wind extending from the Gulf of Mexico into the central United States (Bonner 1968; Bonner et al. 1968). LLJs of this type typically develop to the east of an upper-level baroclinic wave as it moves out of the Rocky Mountains, or along the western periphery of the Bermuda high (Uccellini and Johnson 1979; Chen and Kpaeyeh 1993; Stensrud 1996; Schubert et al. 1998).

The pseudocorrelation map for GDAC2 shows that LLJs in the western Great Plains tend to be confined to the sloping terrain in the lee of the Rocky Mountains. The pseudocorrelation pattern for GDAC2 derived from the reanalysis is broadly similar to that from the NPN, though the west–east gradient is somewhat larger in the reanalysis (Figs. 6a and 6b). This suggests that the horizontal extent of LLJs in the reanalysis is slightly smaller than observed. In the central United States the spatial extent of LLJs is more closely approximated as demonstrated by the similarities of the pseudocorrelation maps for SLAI4 (Figs. 7a and 7b).

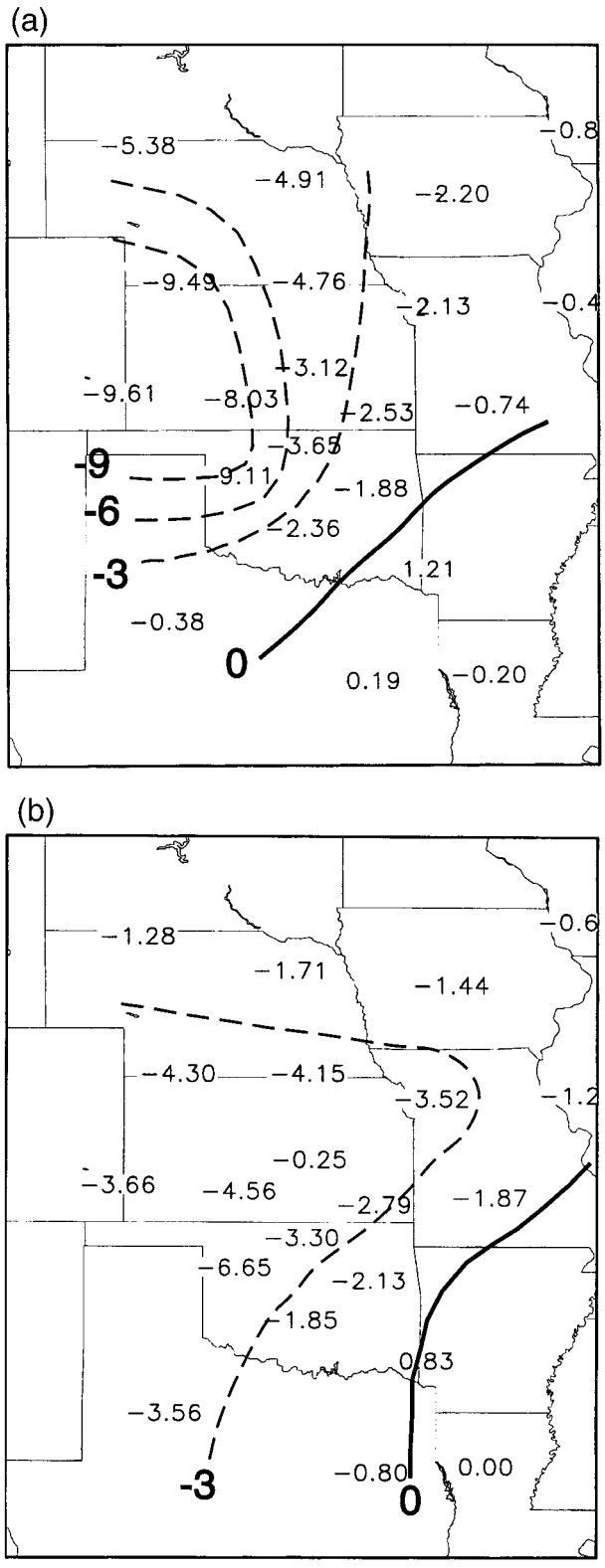

FIG. 5. Summertime LLJ3 station bias (reanalysis minus NPN) at (a) 0600 UTC and (b) 1200 UTC (contour interval is 3%; dashed lines denote negative bias).

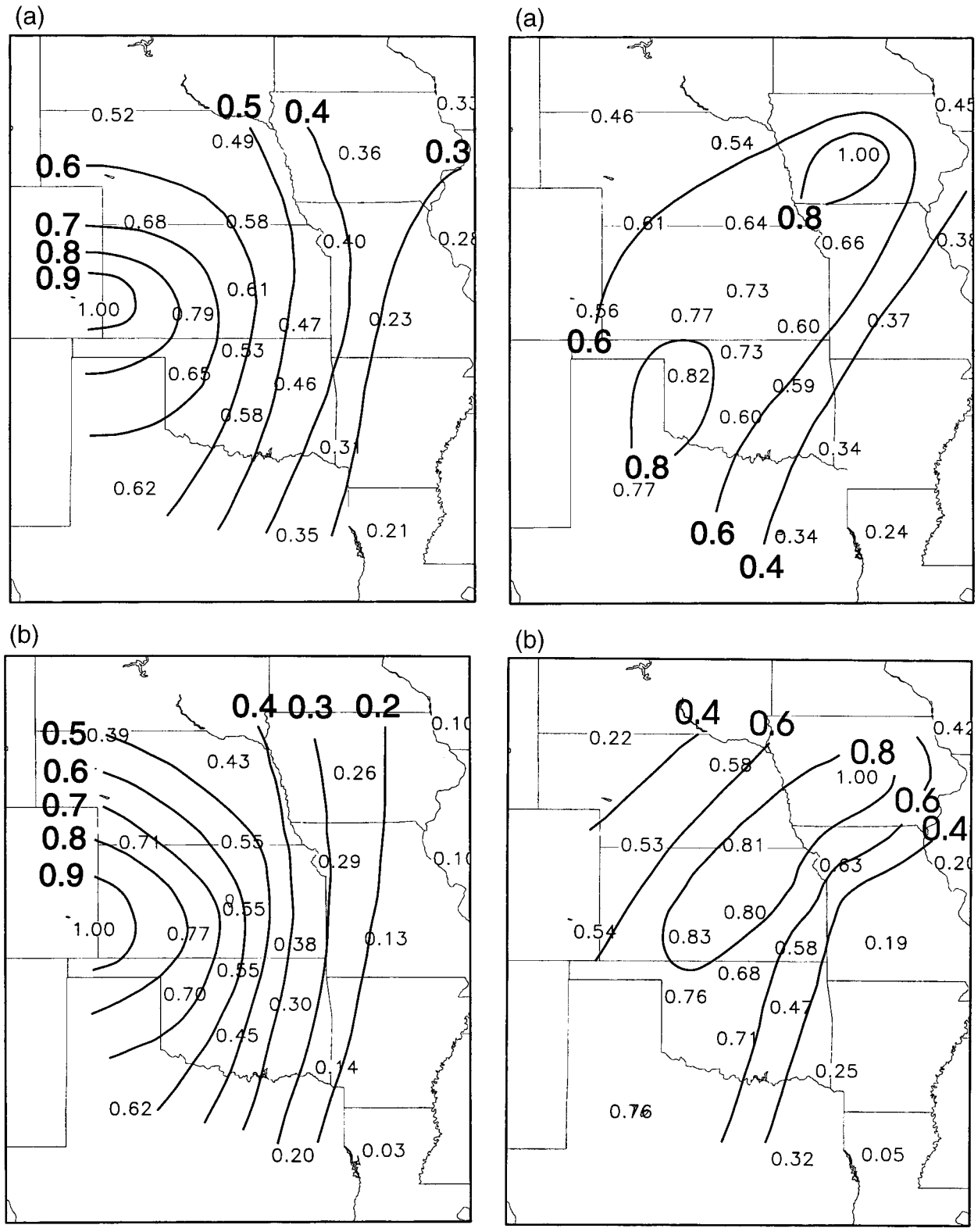

FIG. 6. Pseudocorrelation map generated for GDAC2 at 0600 UTC from the (a) NPN dataset and (b) reanalysis dataset (contour interval is 0.1).

FIG. 7. Pseudocorrelation map generated for SLAI4 at 0600 UTC from the (a) NPN dataset and (b) reanalysis dataset (contour interval is 0.2).

d. Interannual variations of the spatial fields

An advantage of reanalysis data in general is that assessments of interannual variability are less influenced by changes in analysis methodology and perhaps in observational platforms. This remains an advantage so long as bias introduced by the reanalysis technique does not affect interannual variability. Since LLJs have considerable spatial correlation, a scalar measure of interannual variations, such as the variance, is inappropriate. Therefore we defined an empirical orthogonal basis from the spatial distribution of overlapping LLJ1 frequency. The intent is to capture the dominant, spatially coherent year-to-year variations and to determine whether variations in the reanalysis are similar to those observed.

We first determined our empirical orthogonal functions (EOFs) from the NPN dataset and applied a varimax rotation to aid interpretation. We then projected the rotated EOFs onto both the NPN and interpolated reanalysis datasets to obtain time series of principal components. If the interannual deviations from the respective climatological patterns are the same, then the reanalysis time series will overlay that of the NPN. We omit results from 1200 UTC since they are qualitatively similar to those at 0600 UTC.

Most of the variance is captured by the first two EOFs (~75%). The spatial pattern for the coefficients of the first rotated EOF (Fig. 8a) shows that the greatest interannual variability is in the region of the maximum NPN LLJ frequency and indicates that the largest fluctuations are of the maximum LLJ frequency. The spatial pattern of the coefficients for the second rotated EOF (Fig. 8b) exhibits a dipole pattern such that a positive loading indicates LLJs are less frequent in the southern and eastern NPN sites and more frequent in the northern and western NPN sites. Given that summertime LLJs in this region are predominantly southerly, a negative (positive) loading on the second rotated EOF implies enhanced (suppressed) time-mean flow convergence over the Great Plains. The principal component time series (Fig. 9) has large positive weighting on the first rotated EOF and large negative weighting on the second rotated EOF during 1993, when record flooding occurred over the northern Great Plains. The EOF weights suggest that LLJ frequency increased and had a stronger spatial gradient from south to north, resulting in enhanced flow convergence over the central United States. This interpretation is consistent with more detailed analysis of LLJs during the 1993 flood by Arritt et al. (1997) and is supported by the modeling results obtained by Pan et al. (1999), who found a north–south dipole in the low-level wind with opposing sign for the 1988 drought and 1993 flood.

The principal component time series for the reanalysis and the NPN have similar trends but the year-to-year variations are less in the reanalysis series, with the trend line shifted below (above) the NPN series for positive

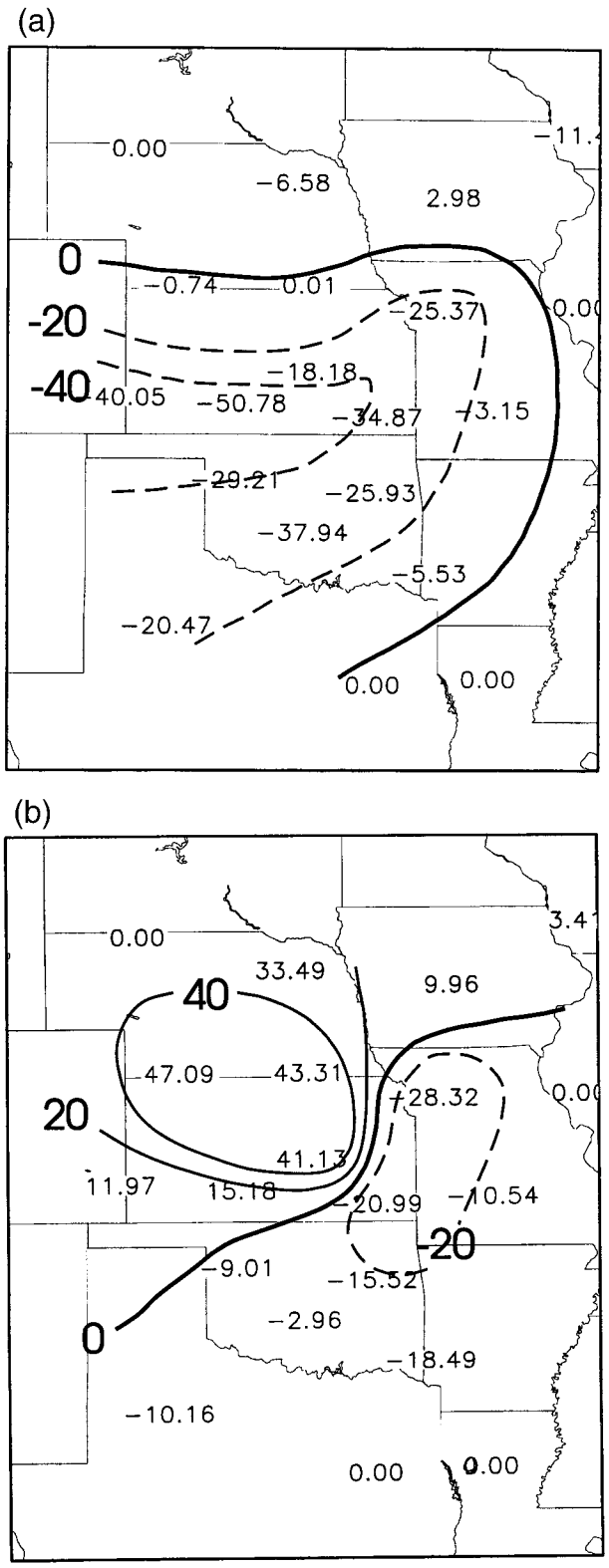

FIG. 8. Spatial pattern of the coefficients of the NPN LLJ1 station frequency for the (a) first rotated EOF and (b) second rotated EOF (contour interval is 20 arbitrary units; dashed lines denote negative coefficients).

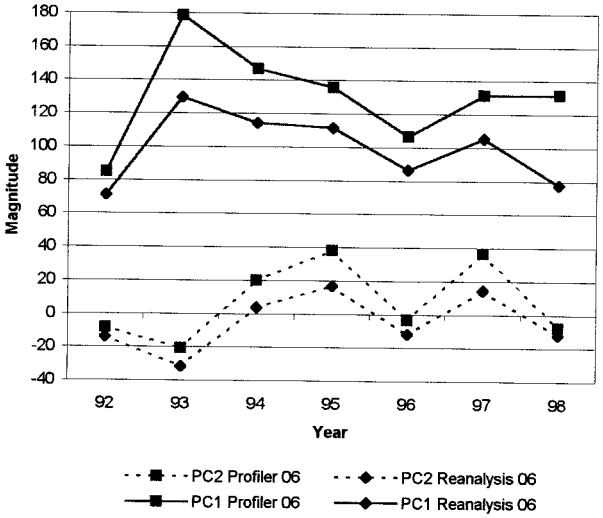

FIG. 9. Time series of the principal components for the first two rotated EOFs.

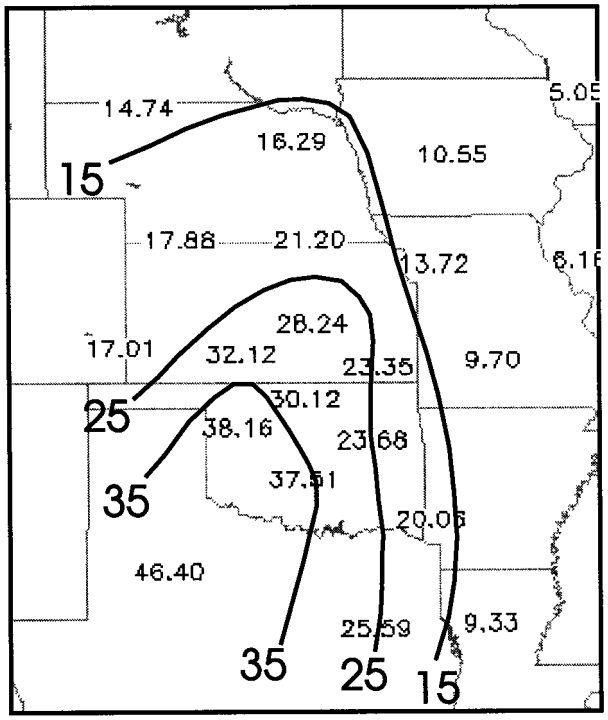

FIG. 10. Reanalysis summertime LLJ1 frequency (1992–98) for 0600 and 1200 UTC combined (contour interval is 10%, beginning with 15%).

(negative) loading (Fig. 9). This suggests that the spatial structure of interannual deviations in the reanalysis is similar but weaker in magnitude than reported by the NPN. We have confirmed this interpretation by manually viewing the deviation maps for each year. A reason for the difference in magnitude may be our choice to use overlapping categories. This introduces the low bias for LLJ3 into the overlapping LLJ1 maps, thus lowering the climatological mean frequency over the entire domain and limiting the magnitude of interannual deviations.

e. Interdecadal change

The long time series of the reanalysis can be used not only for interannual assessments but also for examining changes between decades. We compare our summertime LLJ1 frequency with that for the years 1985–89 reported in Higgins et al. (1997) (their Fig. 7a; we have adopted their contour interval in Fig. 10). Our station frequency maps contain a greater maximum in western Texas and Oklahoma, and a tighter meridional gradient in the central Plains (e.g., their 25% contour extends through eastern Nebraska while ours does not extend past eastern Kansas). This difference may have arisen because our sample was taken from a wetter period over the central United States; note especially that our record includes the record-breaking flood of 1993, while theirs includes the severe drought of 1988. The differences in LLJ frequency and distribution between our period and theirs are consistent with expected low-level wind differences between drought and flood years (Pan et al. 1999; Mo et al. 1997).

f. Mean profiles

To better discern the cause of the low bias in the seasonal LLJ frequency, we defined each wind profile as either misclassified or correctly classified. Correctly classified profiles have the same LLJ category in the NPN and reanalysis datasets. Misclassified profiles are those that fail the criteria of a correctly classified profile. In our sample, most misclassified profiles exhibit a less pronounced peak or no LLJ in the reanalysis dataset when one is present in the profiler dataset. For both misclassified and correctly classified LLJs, we constructed profiles of mean NPN total wind speed and hodographs of the mean NPN total wind; we did the same for the mean reanalysis total wind, geostrophic wind, and ageostrophic wind. The mean wind speed profiles were computed by averaging the wind speed rather than averaging the u and v components. This type of averaging preserves the magnitude but ignores the direction of the wind and is appropriate in the present context since the wind direction is not considered in Bonner's (1968) LLJ criteria. The hodographs, however, are constructed from the mean u and v component wind vectors in order to gain more physical insight regarding the interaction between the geostrophic and ageostrophic components. As examples, we present mean profiles computed for GDAC2. This NPN site is within the region of the largest overall negative bias in the reanalysis (Figs. 3 and 5). Results from other NPN sites that exhibit a low bias are similar so that the mean profiles at GDAC2 are representative.

1) 0600 UTC

For misclassified LLJs, mean total wind speed in the reanalysis has a low-level maximum (Fig. 11a), but it is severely underestimated and occurs slightly aloft of the NPN maximum (698 compared to 500 m). In contrast, the local wind speed minimum above the low-level maximum (and the wind profile above this level) is remarkably similar to the NPN observations, having the same magnitude and occurring at nearly the same level.

The influence of the analysis scheme is determined by comparing mean profiles of the unadjusted 6-h forecast valid at 0600 UTC (Figs. 11c and 11d) to those of the final analysis (Figs. 11a and 11b). A less pronounced peak is evident in the mean total wind speed from the 6-h forecast (about 3 m s^{-1} less; Fig. 11c), because the v component in the mean total wind speed is less (Fig. 11d). Near the surface the mean ageostrophic wind shifts from west-northwesterly to southeasterly and approaches a southerly orientation by 1000 m (compare Fig. 11b to 11d). The mean ageostrophic wind speed increases more in the layer from the surface to 1000 m than the mean geostrophic wind speed. Therefore, one effect of the analysis scheme is to increase low-level ageostrophic motion.

Analytical, observational, and numerical experiments suggest that the dominant process in LLJ formation over the Great Plains is the inertial acceleration of an ageostrophic wind vector so that it becomes aligned with the geostrophic wind vector (Blackadar 1957; Bonner and Paegle 1970; Parish et al. 1988; Zhong et al. 1996). One possibility for the erroneous mean profiles of total wind from the 6-h forecast is that the ageostrophic wind in the initial condition may be erroneous. Mean profiles generated from the 0000 UTC analysis indicate a tendency to underestimate the total wind speed (Figs. 11e and 11f); however, the ageostrophic wind speed is relatively large. Below 1000-m the mean ageostrophic wind speed from the 6-h forecast valid at 0600 UTC (Fig. 11c) is diminished to almost half of its 0000 UTC magnitude (Fig. 11e) and exhibits a weak northerly component (Fig. 11d). After adjustments by the analysis scheme at 0600 UTC the mean ageostrophic wind speed increases (Fig. 11a), and the orientation of the mean ageostophic wind between 500 and 1000 m is rotated about 110° clockwise of its direction at 0000 UTC (compare Figs. 11f and 11b). Note that a purely inertial acceleration at GDAC2 (37.77°N) over 6 h results in a clockwise rotation of about 110°.

Similar tendencies are evident in mean profiles for correctly categorized LLJs (Fig. 12). One difference that may contribute to proper classification of these LLJs is that the low-level mean ageostrophic wind speed is increased more than in the misclassified profiles (2 m s^{-1} increase from Figs. 11c to 11a compared to 3 m s^{-1} from Figs. 12c and 12a). The similarities, however, are of most interest since they suggest that tendency toward excessive geostrophic balance in the GCM prediction might be a reason for the low bias in LLJ frequency.

2) 1200 UTC

At 1200 UTC the reanalysis mean total wind speed is peaked just below 1000 m and is slightly greater than the geostrophic wind speed (Fig. 13a). Between 500 and 1000 m the ageostrophic wind speed decreases, and its orientation changes from nearly parallel to slightly opposing the mean geostrophic wind (Figs. 13a and 13b). Both the geostrophic and ageostrophic wind speed are less than in the 6-h forecast (a decrease of about 3 m s^{-1} in the ageostrophic and 1 m s^{-1} in the geostrophic wind, Figs. 13c and 13a); however, the total wind speed is greater than in the forecast because the geostrophic and ageostrophic components reinforce rather than oppose one another (Figs. 13d and 13b). Correctly classified profiles at 1200 UTC (Fig. 14) display very small differences between the 6-h forecast and the final analysis. A more in-depth analysis, possibly including composite maps of low-level geopotential height and low-level wind, is necessary to ascertain the source of extreme error in the mean profiles for the misclassified LLJs. It appears, however, that the analysis is forced to make an adjustment in the opposite sense to that at 0600 UTC; that is, a more geostrophic state is obtained by the analysis scheme.

4. Discussion

Consistent with other evaluations, we find that the climatological maximum LLJ1 frequency in the re-

→

FIG. 11. For misclassified LLJs at 0600 UTC (a) profile of mean for NPN total wind speed (open square) and reanalysis total (filled diamond), and geostrophic (solid line) and ageostrophic wind speed (dashed line). (b) Hodograph of mean u and v components for NPN total wind (open squares) and reanalysis total (filled diamonds), and geostrophic (solid line) and ageostrophic wind (dashed line). Bold and italicized numbers indicate the mean height of the lowest data point, the maximum total wind (marked with an **M**), and the levels nearest 1000, 1500, and 3000 m. (c) Profile of mean for NPN total wind speed (open squares) and **6-h forecast** of total (filled diamonds), geostrophic (solid line), and ageostrophic wind speed (dashed line). (d) Hodograph of mean u and v components for NPN total wind (open squares) and **6-h forecast** of total (filled diamonds), geostrophic (solid line), and ageostophic wind (dashed line). The bold and italicized numbers function identically to those in (b). (e) Profile of mean for NPN total wind speed (open square) and **0000 UTC reanalysis** of total (filled diamond), geostrophic (solid line), and ageostrophic wind speed (dashed line). (f) Hodograph of mean u and v components for NPN total wind (open squares) and **0000 UTC reanalysis** of total (filled diamonds), geostrophic (solid line), and ageostophic wind (dashed line). The bold and italicized numbers function identically to those in (b).

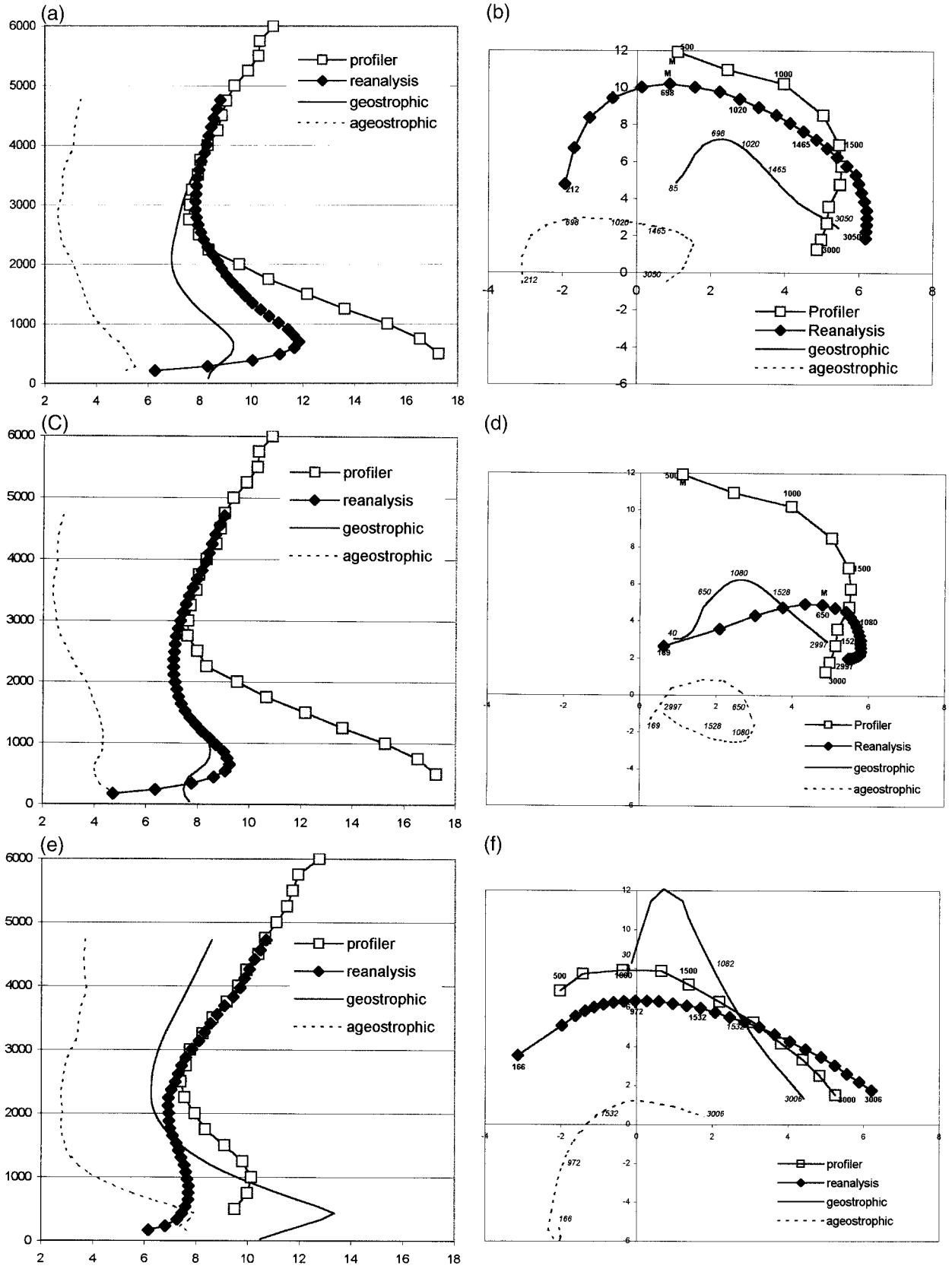

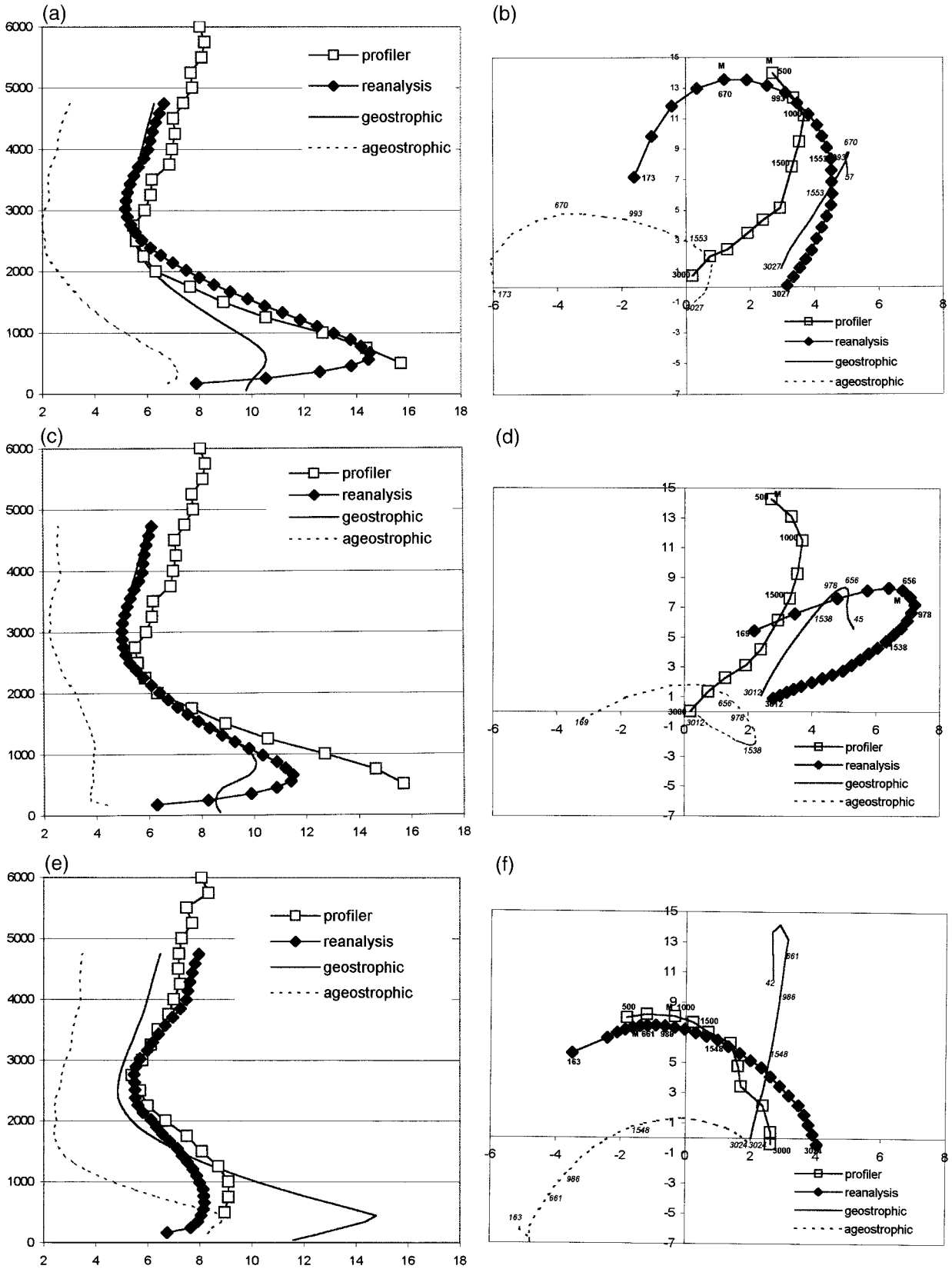

FIG. 12. Same as Fig. 11 except for correctly classified LLJs at 0600 UTC.

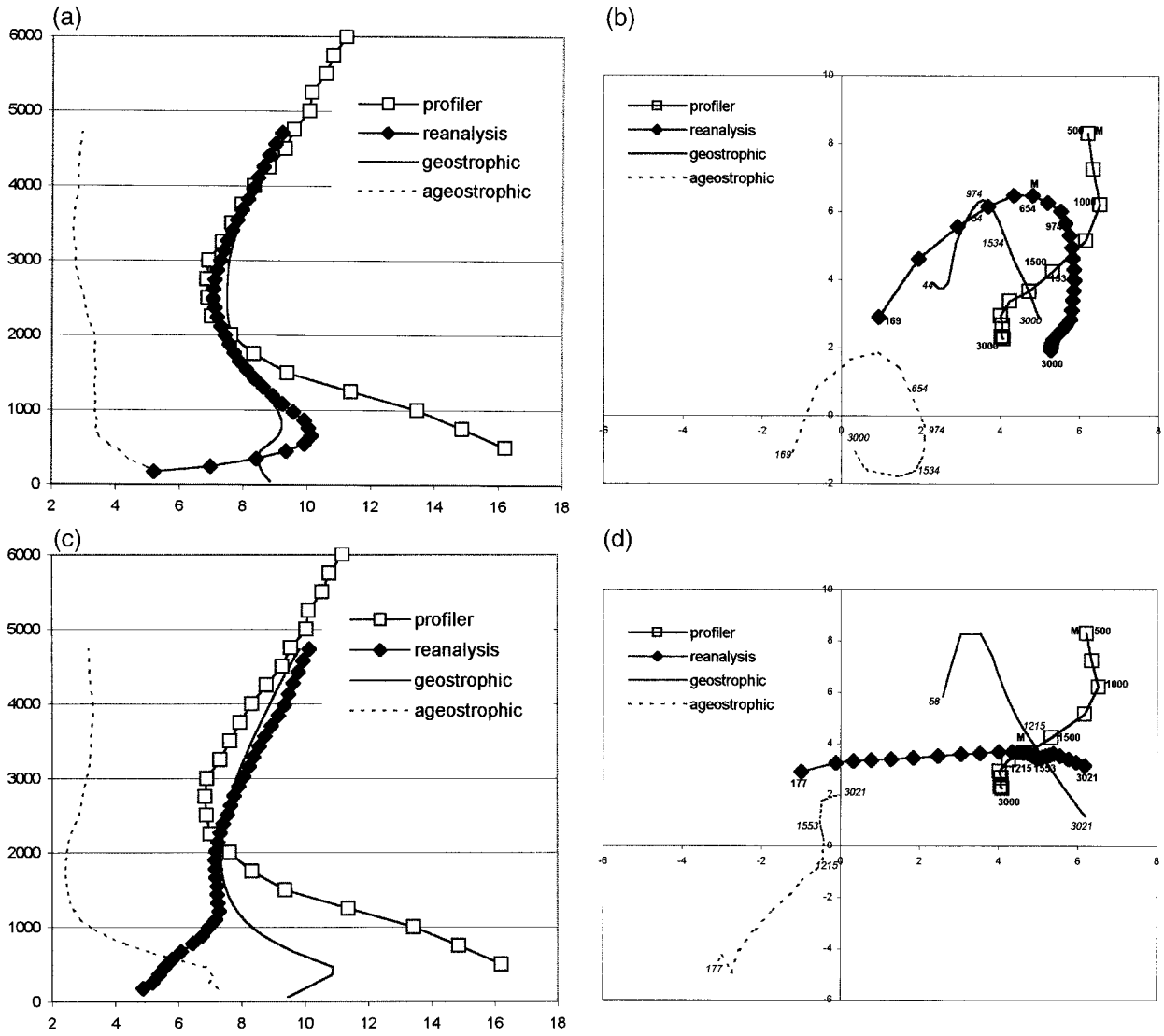

FIG. 13. Same as Figs. 11a–d except for misclassified LLJs at 1200 UTC.

analysis is about the same as observed. However, the orientation of the station bias gradient for both LLJ1 and LLJ3 suggests that the terrain forcing in the lee of the Rocky Mountains is deficient. Previous comparisons of the output from data assimilation systems reveal large discrepancies in moisture flux and moisture flux divergence in regions where terrain–atmosphere interaction plays a prominent role in the evolution of the low-level flow (see, e.g., Higgins et al. 1996). The estimated low-level wind contributes more to these differences than does the estimated moisture (Higgins et al. 1996; Min and Schubert 1997). Our results suggest that part of the wind error may result from an inadequate depiction of the inertial acceleration of the low-level ageostrophic wind.

Simply increasing the horizontal resolution of the GCM might not improve the prediction of total wind in the lee of the Rocky Mountains. Summertime LLJ frequency in the central United States is robust with respect to changes in horizontal resolution (Ghan et al. 1996), but LLJ development is sensitive to the representation of terrain slope (McNider and Pielke 1981; Savajari 1991; Holton 1967). We suggest independent tests of the sensitivity of LLJ formation to terrain resolution and horizontal grid spacing in GCMs, much like the sensitivity study performed by Zhong et al. (1996) for a high-resolution mesoscale model.

An unresolved question is: why does the reanalysis (and most GCMs) fail to capture the nocturnal maximum in summertime precipitation over the Great Plains even though they contain a generally realistic representation of LLJs? We propose two hypotheses. First, the inability of the GCM to realistically sustain the ageostrophic wind speed (and thus the divergent component of the

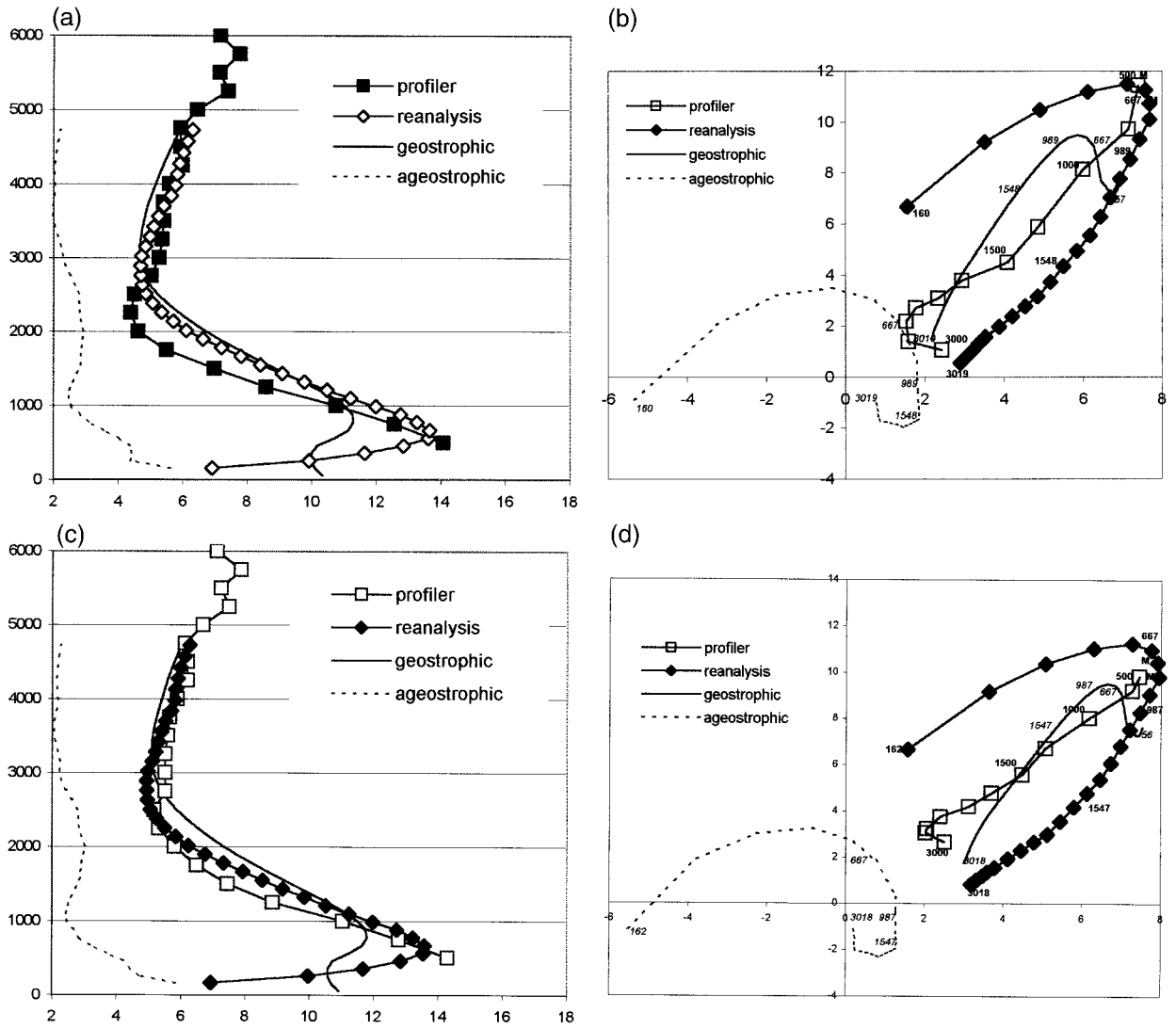

FIG. 14. Same as Figs. 11a–d except for correctly classified LLJs at 1200 UTC.

wind) between 0000 UTC and 0600 UTC may diminish the likelihood that the convective parameterization scheme is invoked. Second, the cumulus parameterizations in most GCMs are unable to represent organized mesoscale precipitation systems, especially mesoscale convective complexes (MCCs). MCCs and other large MCSs (Fritsch et al. 1986; Anderson and Arritt 1998) produce more than half of the nocturnal precipitation in the central United States. These systems are of subgrid scale in present-day GCMs and therefore must be parameterized rather than explicitly resolved; however, MCCs are dynamically organized and long-lived, in contrast to the quasi-random convective elements usually assumed in cumulus parameterizations. [The discussion by Frank (1983) is relevant here.] One way to test this hypothesis is to perform simulations with a regional climate model at various resolutions, comparing results for grids fine enough to resolve MCCs and too coarse to resolve MCCs.

5. Conclusions

A comparison of summertime LLJs in the reanalysis to those in the NPN, an independent dataset, yields the following results:

- Even though constrained by observations the reanalysis LLJ1 frequency is somewhat lower than in the NPN climatology; the latter itself is lower than in high-resolution rawinsonde data. Strong LLJs [category 3 in Bonner (1968)] in the reanalysis are infrequent everywhere and almost never occur in the northern Great Plains.
- Interannual variability of overlapping LLJ1 frequency is slightly less in the reanalysis than in the NPN.

- Over the central United States, the spatial extent of LLJs in the reanalysis nearly matches that of the NPN, while in the lee of the Rocky Mountains LLJs in the reanalysis are slightly less extensive than observed by the NPN.
- By 0600 UTC the GCM prediction tends to approach a greater degree of geostrophic balance than is observed for LLJs in the lee of the Rocky Mountains. Introduction of observed data tends to restore the ageostrophic component.
- At 1200 UTC, the analysis scheme frequently adjusts the predicted low-level flow in the lee of the Rocky Mountains toward geostrophic balance for miscategorized LLJs; 6-h forecasts for correctly categorized LLJs require relatively minor adjustments.

Acknowledgments. This research was sponsored by National Science Foundation Grants ATM-9616728 and ATM-9627890. This is Journal Paper No. J-18448 of the Iowa Iowa Agriculture and Home Economics Experiment Station, Ames, Iowa, Project No. 3245, and supported by Hatch Act and State of Iowa. We thank Dennis Todey for his assistance with figure preparation. This manuscript was improved significantly by the comments of two anonymous reviewers.

REFERENCES

Anderson, C. J., and R. W. Arritt, 1998: Mesoscale convective complexes and persistent elongated convective systems over the United States during 1992 and 1993. *Mon. Wea. Rev.,* **126,** 578–599.

Arritt, R. W., T. D. Rink, M. Segal, D. P. Todey, C. A. Clark, M. J. Mitchell, and K. M. Labas, 1997: The Great Plains low-level jet during the warm season of 1993. *Mon. Wea. Rev.,* **125,** 2176–2192.

Barth, M. F., R. B. Chadwick, and D. W. van de Kamp, 1994: Data processing algorithms used by NOAA's wind profiler demonstration network *Ann. Geophys.,* **12,** 518–528.

Blackadar, A. K., 1957: Boundary layer wind maxima and their significance for the formation of nominal inversions. *Bull. Amer. Meteor. Soc.,* **38,** 283–290.

Bonner, W. D., 1968: Climatology of the low level jet. *Mon. Wea. Rev.,* **96,** 833–850.

——, and J. Paegle, 1970: Diurnal variation in boundary layer winds over the south-central United States in summer. *Mon. Wea. Rev.,* **98,** 735–744.

——, S. Esbensen, and R. Greenberg, 1968: Kinematics of the low-level jet. *J. Appl. Meteor.,* **7,** 339–347.

Chen, T.-C., and J. A. Kpaeyah, 1993: The synoptic-scale environment associated with the low-level jet of the Great Plains. *Mon. Wea. Rev.,* **121,** 416–420.

Daniel, C. J., R. W. Arritt, and C. J. Anderson, 1999: Accuracy of 404-MHz radar profilers for detection of low level jets over the central United States. *J. Appl. Meteor.,* **38,** 1391–1396.

Frank, W. M., 1983: The cumulus parameterization problem. *Mon. Wea. Rev.,* **111,** 1859–1871.

Fritsch, J. M., R. J. Kane, and C. R. Chelius, 1986: The contribution of mesoscale convective weather systems to the warm-season precipitation in the United States. *J. Climate Appl. Meteor.,* **25,** 1333–1135.

Ghan, S. J., X. Bian, and L. Corsetti, 1996: Simulation of the Great Plains low-level jet and associated clouds by general circulation models. *Mon. Wea. Rev.,* **124,** 1388–1408.

Helfand, H. M., and S. D. Schubert, 1995: Climatology of the simulated Great Plains low-level jet and its contribution to the continental moisture budget of the United States. *J. Climate,* **8,** 784–806.

Higgins, R. W., K. C. Mo, and S. D. Schubert, 1996: The moisture budget of the central United States in spring as evaluated in the NCEP/NCAR and the NASA/DAO reanalyses *Mon. Wea. Rev.,* **124,** 939–963.

——, Y. Yao, E. S. Yaresh, J. E. Janowiak, and K. C. Mo, 1997: Influence of the Great Plains low-level jet on summertime precipitation and moisture transport over the central United States. *J. Climate,* **10,** 481–507.

Holton, J. R., 1967: The diurnal boundary layer wind oscillation above sloping terrain. *Tellus,* **19,** 199–205.

Kalnay, E., and Coauthors, 1996: The NCEP/NCAR 40-Year Reanalysis Project. *Bull. Amer. Meteor. Soc.,* **77,** 437–471.

Maddox, R. A., 1983: Large-scale meteorological conditions associated with midlatitude, mesoscale convective complexes. *Mon. Wea. Rev.,* **111,** 1475–1493.

McNider, R. T., and R. A. Pielke, 1981: Diurnal boundary-layer development over sloping terrain. *J. Atmos. Sci.,* **38,** 2198–2212.

Min, W., and S. Schubert, 1997: The climate signal in regional moisture fluxes: A comparison of three global data assimilation products. *J. Climate,* **10,** 2623–2642.

Mitchell, M. J., R. W. Arritt, and K. Labas, 1995: A climatology of the warm season Great Plains low-level jet using wind profiler observations. *Wea. Forecasting,* **10,** 576–591.

Mo, K. C., J. N. Paegle, and R. W. Higgins, 1997: Atmospheric processes associated with summer floods and droughts in the central United States. *J. Climate,* **10,** 3028–3046.

Pan, Z., M. Segal, R. W. Arritt, T.-C. Chen, and S.-P. Weng, 1999: A method for simulating effects of quasi-stationary wave anomalies on regional climate. *J. Climate,* **12,** 1336–1343.

Parish, T. R., A. R. Rodi, and R. D. Clark, 1988: A case study of the summertime Great Plains low level jet. *Mon. Wea. Rev.,* **116,** 94–105.

Savajari, H., 1991: The United States Great Plains diurnal ABL variation and the nocturnal low-level jet. *Mon. Wea. Rev.,* **119,** 833–840.

Schubert, S. D., H. M. Helfand, C.-Y. Wu, and W. Min, 1998: Subseasonal variation in warm-season moisture transport and precipitation over the central and eastern United States. *J. Climate,* **11,** 2530–2555.

Stensrud, D. J., 1996: Importance of low-level jets to climate: A review. *J. Climate,* **9,** 1698–1711.

Uccellini, L. W., and D. R. Johnson, 1979: The coupling of upper and lower level jet streaks and implications for the development of severe convective storms. *Mon. Wea. Rev.,* **107,** 682–703.

Whiteman, C. D., X. Bian, and S. Zhong, 1997: Low-level jet climatology from enhanced rawinsonde observations at a site in the southern Great Plains. *J. Appl. Meteor.,* **36,** 1363–1376.

Wilczak, J. M., and Coauthors, 1995: Contamination of wind profiler data by migrating birds: Characteristics of corrupted data and potential solutions. *J. Atmos. Oceanic Technol.,* **12,** 449–467.

Zhong, S., J. D. Fast, and X. Bian, 1996: A case study of the Great Plains low-level jet using wind profiler network data and a high-resolution mesoscale model. *Mon. Wea. Rev.,* **124,** 785–806.